

First β^- -decay spectroscopy study of ^{157}Nd

D. J. Hartley¹, F. G. Kondev², M. P. Carpenter², J. A. Clark^{2,3}, P. Copp², B. Kay²,
T. Lauritsen², G. Savard^{2,4}, D. Seweryniak², G. L. Wilson^{2,5} and J. Wu^{2,*}

¹*Department of Physics, U.S. Naval Academy, Annapolis, Maryland 21402, USA*

²*Physics Division, Argonne National Laboratory, Lemont, Illinois 60439, USA*

³*Department of Physics and Astronomy, University of Manitoba, Winnipeg, Manitoba R3T 2N2, Canada*

⁴*Department of Physics, University of Chicago, Chicago, Illinois 60637, USA*

⁵*Department of Physics and Astronomy, Louisiana State University, Baton Rouge, Louisiana 70803, USA*



(Received 9 May 2023; revised 10 July 2023; accepted 26 July 2023; published 14 August 2023)

As part of an effort to better understand the structure of neutron-rich, rare-earth nuclei that are involved in the r process, an experiment aimed at the β^- -decay spectroscopy of ^{157}Nd was performed. The CARIBU source provided an isobarically separated $A = 157$ beam which was delivered to the SATURN decay station at Argonne National Laboratory. A half-life of $t_{1/2} = 1.17(4)$ s was measured for the ^{157}Nd decay, which is in agreement with a previously reported value. A level scheme based on the ^{157}Nd β^- decay was established for the first time. The level at 1703 keV in the daughter ^{157}Pm nucleus was assigned the $\pi 7/2[523]$ configuration and it was found to be populated quite strongly as a result of an allowed-unhindered “spin-flip” transition from the $\nu 5/2[523]$ ground state in ^{157}Nd .

DOI: [10.1103/PhysRevC.108.024307](https://doi.org/10.1103/PhysRevC.108.024307)

I. INTRODUCTION

The Californium Rare Isotope Breeder Upgrade (CARIBU) facility [1] at Argonne National Laboratory has made it possible to explore the neutron-rich isotopes in the rare-earth region of the nuclear chart. Indeed, new mass measurements [2–5] using the Canadian Penning Trap have provided nuclear astrophysicists with needed information to better understand the rare-earth peak in the abundance distribution [6–9]. Additionally, these measurements have identified long-lived isomers that are of great interest to nuclear structure physicists. Our collaboration is now focused on β^- -decay spectroscopy studies of these isotopes in order to measure the half-lives of the ground states and isomers (which are also beneficial for astrophysical models) and to elucidate their structure, together with the structure of levels populated in the daughter nuclei.

In the present work, β^- decay of ^{157}Nd was studied, which possesses seven more neutrons than the heaviest stable neodymium isotope. The half-life of this nucleus was recently measured for the first time at the RIKEN facility [10], and the present study confirms that value. In addition, 11 excited levels in the daughter nucleus ^{157}Pm , populated in β^- decay of ^{157}Nd , were established. Nilsson configurations are proposed for some of the levels, based on excitation-energy systematics of known quasiparticle states in nearby nuclei and the observed $\log ft$ values.

II. EXPERIMENTAL DETAILS

The CARIBU source [1] provided an isobarically separated $A = 157$ beam that was delivered to the SATURN moving tape collection system [11], where ^{157}Nd was observed to be the most neutron-rich isotope in this mass selection. The X-Array spectrometer comprised of five germanium clover detectors to observe emitted γ rays and plastic scintillator detectors for triggering on β^- particles [11] surrounded SATURN. A digital acquisition system recorded the energy and time information of these detectors, where the timing information utilized a 100 MHz clock. Several different tape cycles were employed based on the previously reported ^{157}Nd half-life of $t_{1/2} = 1.15(3)$ s [10]. In each case a 3 s growth time (beam on), a decay time (beam off), 2 s tape movement, and 1 s background accumulation was used. Decay time (beam off) periods of 4 s, 6 s, and 12 s were selected during the experiment in order to better identify the optimal setting to observe ^{157}Pm γ rays. Background measurements using longer tape cycles (94 s beam on/200 s beam off and 600 s beam on/600 s beam off), as well as room background collection, were also carried out. A β^- -gated, E_γ vs. time coincidence matrix was constructed from the 6 s decay time data set and it was used to determine the half-life of ^{157}Nd .

In order to study the excited levels in the ^{157}Pm daughter nucleus, β^- -gated E_γ - E_γ coincidence histograms were also constructed for each of the three data sets using both the beam-on and beam-off portions. The longer-lived background was subtracted from these matrices which were added together. A total of approximately 1.9×10^6 β^- - γ - γ coincidence events were recorded in the summed matrix. Energy calibration and efficiency parameters were determined with selected

*Present address: National Nuclear Data Center, Brookhaven National Laboratory, Upton, New York 11973, USA.

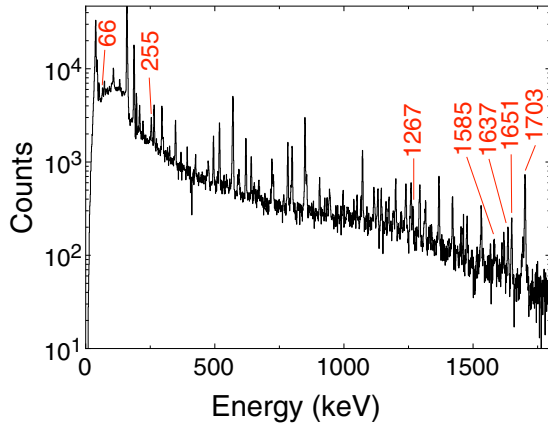


FIG. 1. Spectrum of coincident γ rays with β^- particles during the beam-off portion of the 3 s growth/6 s decay data set. The marked peaks are associated with the decay of ^{157}Nd .

transitions from ^{56}Co , ^{152}Eu , ^{182}Ta , and ^{243}Am sources. In addition, an internal efficiency at low energies was included by using γ rays from the ^{157}Pm decay present in the data (see Fig. 1), as well as transitions from the longer lived ^{157}Sm decay.

III. EXPERIMENTAL RESULTS

Previously, the half-life of ^{157}Nd had been reported [10] using time differences between implanted ions and detected β^- particles. However, no states in the daughter nucleus, ^{157}Pm , populated by the β^- decay of ^{157}Nd were published. A rotational sequence based on the proposed $J^\pi = (5/2^-)$ ground state was assigned to ^{157}Pm by Bhattacharyya *et al.* [12], which was observed up to $(27/2^-)$.

The γ rays in coincidence with β^- particles during the beam-off portion of the 6 s decay time data are presented in Fig. 1. Nearly all of the unmarked peaks are attributed to the $^{157}\text{Pm} \rightarrow ^{157}\text{Sm}$ decay, which dominates the spectrum. However, the γ rays denoted with energy values in Fig. 1 display lifetimes that are consistent with the ^{157}Nd decay into ^{157}Pm , or they were found to be in coincidence with transitions that could be identified with ^{157}Pm .

In order to measure the lifetime of the ^{157}Nd ground state, gates on the strongest and cleanest γ transitions associated with ^{157}Pm were placed in the E_γ vs. time coincidence matrix. Gates on the 1637-, 1651-, and 1703-keV transitions were individually background subtracted and then added together to produce the time spectrum shown in Fig. 2. A single-exponential fit to the decay portion was performed resulting in a half-life measurement of $t_{1/2} = 1.17(4)$ s, which is in agreement with the previous value of Ref. [10].

The E_γ - E_γ coincidence matrix was analyzed and it should be noted that several of the transitions in Fig. 1 (1651 and 1703 keV) were not observed in these data. This indicates that these transitions decay directly to the ground state of ^{157}Pm . A coincidence gate on the 66-keV γ ray produced the spectrum shown in the inset of Fig. 3. Note that the authors of Ref. [12] placed the 66-keV line in the ^{157}Pm level scheme, and the present data confirm their assignment. When adding

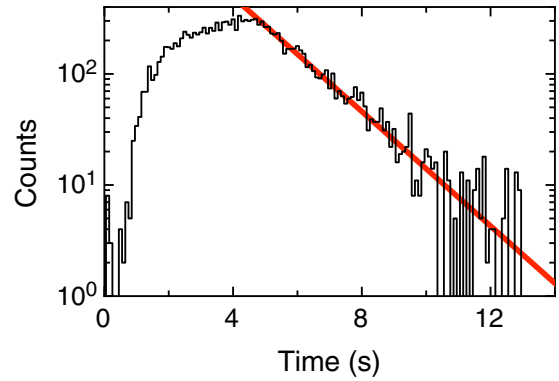


FIG. 2. Time spectrum resulting from gates set on the 1637-, 1651-, and 1703-keV γ rays. The red solid line is a single-exponential fit to the data which yields a half-life of 1.17(4) s.

the energies of the 66-keV transition to the 1637- and 1585-keV ones, the summations give the same values as the 1703- and 1651-keV γ rays, respectively, which are seen in Fig. 1. This strongly implies energy levels exist at these latter values, which are drawn in Fig. 4. In addition, the clear coincidence with the 1529-keV line (see inset of Fig. 3) establishes the level at 1595 keV.

The main portion of Fig. 3 displays the transitions that are in coincidence with the 255-keV γ ray, which was found to be one of the strongest ^{157}Pm lines in Fig. 1. This transition is not in coincidence with the 66-keV γ ray, but note it is in coincidence with a 1448-keV transition. The sum of 255 keV and 1448 keV also results in 1703 keV, which further provides evidence of the 1703-keV state. In addition, based on the relative strengths of the 255- and 1448-keV lines, it is likely that the 255-keV transition directly feeds the ground state, and the other coincident γ rays observed in Fig. 3 result from higher lying states feeding the 255-keV level, as seen in Fig. 4. The coincidences of this 255-keV γ ray with the 441-, 495-, 1014-, 1057-, 1174-, and 1986-keV transitions led to the assignment of levels at energies of 695, 750, 1269, 1311, 1429, and 2241 keV, respectively. It should be noted that a

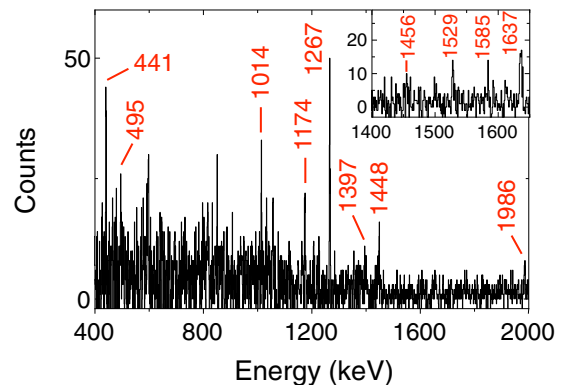


FIG. 3. The main spectrum displays transitions in coincidence with the 255-keV γ ray. The inset shows the high-energy portion of the spectrum displaying γ rays that are in coincidence with the known 66-keV transition in ^{157}Pm .

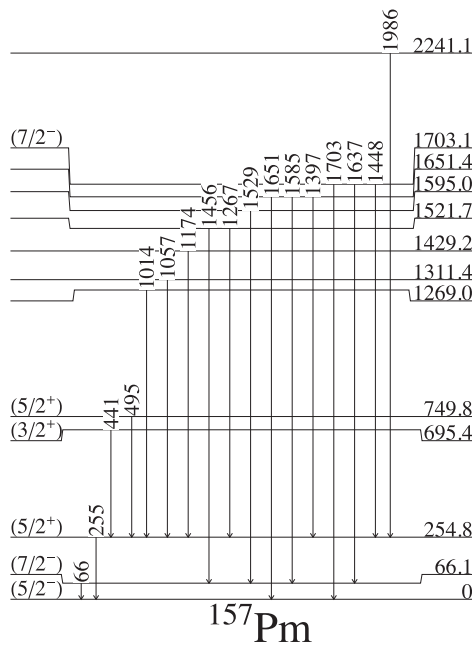


FIG. 4. Level scheme of ^{157}Pm resulting from the decay of ^{157}Nd . All states above the 66-keV level are newly identified. When possible, tentative spin and parity assignments have been made. The spin and parity of the ^{157}Nd parent state is $(5/2^-)$.

level at 254 keV was identified in Ref. [12] as the spin $11/2$ member of a rotational band based on the $h_{11/2}$ quasiproton. The 255-keV state in Fig. 4 is clearly not the same level as the one at 254 keV in Ref. [12] as they do not share the same γ decays from their respective levels.

When possible, the intensities of the transitions shown in Fig. 4 were determined from the β^- -gated γ -ray singles spectrum shown in Fig. 1. For weaker transitions, relative intensities were obtained from the coincidence matrix and then normalized with a γ ray whose intensity was determined from Fig. 1. Once these intensities were measured, this information was used to calculate the β^- feeding intensity into each level using intensity balance considerations, and subsequently the $\log ft$ values were determined. These values are only approximate due to the fact that the feeding of the ^{157}Pm ground state could not be directly measured. Instead, an approximate I_β was obtained by reviewing the $\log ft$ values of the $\nu 5/2[523] \rightarrow \pi 5/2[532]$ decays in the nearby isotones ^{159}Sm and ^{161}Gd . A value of $I_\beta \approx 10\%$ was determined by adopting $\log ft = 5.8$, which is the average of the two values from ^{159}Sm ($\log ft = 5.6$) [13] and ^{161}Gd ($\log ft = 6.0$) [14]. The f value was calculated using the LOGFT code [15] and the recommended $Q_{\beta^-}(^{157}\text{Nd}) = 5803(7)$ keV from AME2020 [16]. Table I provides the energies of the levels, the proposed J^π values, the γ -ray energies and intensities, as well as the I_β intensities and $\log ft$ values.

IV. DISCUSSION

The ground state of ^{157}Nd was tentatively assigned as $J^\pi = (5/2^-)$ in Refs. [17,18] based on the expected $\nu 5/2[523]$ Nilsson orbital. This is in agreement with the firm assignments

TABLE I. Level energies, J^π and $\log ft$ values, γ -ray energies and intensities for the states fed in ^{157}Pm resulting from the β^- decay of ^{157}Nd which has $J^\pi = (5/2^-)$.

E_{level} (keV)	J^π	I_β^a (%)	$\log ft$	E_γ^b (keV)	I_γ^c (rel. units)
0	$(5/2^-)$	≈ 10	≈ 5.8		
66.1	$(7/2^-)$	≈ 48	≈ 5.1	66.1	5000(400)
254.8	$(5/2^+)$	≈ 1.5	≈ 6.5	254.8	6420(420)
695.4	$(3/2^+)$	≈ 1.2	≈ 6.5	440.6	670(140)
749.8	$(5/2^+)$	≈ 0.9	≈ 6.6	495.0	490(90)
1269.0		≈ 1.3	≈ 6.2	1014.2	710(140)
1311.4		≈ 0.9	≈ 6.4	1056.6	510(110)
1429.2		≈ 1.4	≈ 6.1	1174.4	745(150)
1521.7		≈ 4.1	≈ 5.6	1455.7	630(120)
				1266.9	1650(260)
1595.0		≈ 1.7	≈ 6.0	1528.9	960(180)
1651.4		≈ 6.1	≈ 5.4	1651.4	2350(240)
				1585.3	730(140)
1703.1	$(7/2^-)$	≈ 22	≈ 4.8	1703.1	10000(300)
				1637.0	1780(220)
				1448.3	355(70)
2241.1		≈ 0.7	≈ 6.1	1986.3	360(70)

^aValues deduced from total intensity balances at each level. Note that the 66.1-keV transition was assumed to have pure $M1$ multipolarity.

^bValues accurate within ± 0.5 keV.

^cRelative intensity normalized to $I_\gamma(1703.1\gamma) = 10000$.

of $J^\pi = 5/2^-$, $\nu 5/2[523]$ for the ground states of the $N = 97$ isotones ^{159}Sm [13], ^{161}Gd [14], and ^{163}Dy [19]. The ground state of ^{157}Pm was tentatively assigned $J^\pi = (5/2^-)$ and the $\pi 5/2[532]$ configuration in the latest ENSDF evaluation [20], which agrees with the systematics of ground states for the nearest $Z = 61$ nuclei $^{153,155}\text{Pm}$ [21,22].

The first excited state in ^{157}Pm is based on the rotational excitation of the ground state as it was previously observed in the high-spin study of Ref. [12]. The new state at 255 keV, as seen in Fig. 4, was primarily fed by γ transitions rather than direct β decay. It only decays to the ground state; therefore, it could have spin/parity values of $3/2^\pm$, $5/2^\pm$, $7/2^\pm$, or $9/2^-$. Figure 5 displays the energies of the quasiproton orbitals that are well known to be near the Fermi surfaces of the $N = 90, 92, 94$, and 96 promethium, europium, and terbium nuclei. In this figure, the ground states of the promethium, europium, and terbium isotopes were arbitrarily set at 800 keV, 1000 keV, and 1200 keV, respectively, in order to better observe the trends of these Nilsson states. As seen in Fig. 5, the $\pi 5/2[413]$ orbital lies very close to the $\pi 5/2[532]$ one and if the 255-keV level is associated with the former, it fits with the systematic trend observed in the promethium isotopes. Therefore, it is likely that the 255-keV state has $J^\pi = (5/2^+)$ and is based on the $\pi 5/2[413]$ orbital, but this is a tentative assignment until further experimental evidence is observed.

The next highest state is located at an energy of 695 keV where only a single transition (441 keV) is observed to depopulate the level. This transition feeds the proposed $5/2^+$ level discussed above. As seen in Fig. 5, the $\pi 3/2[411]$ orbital is

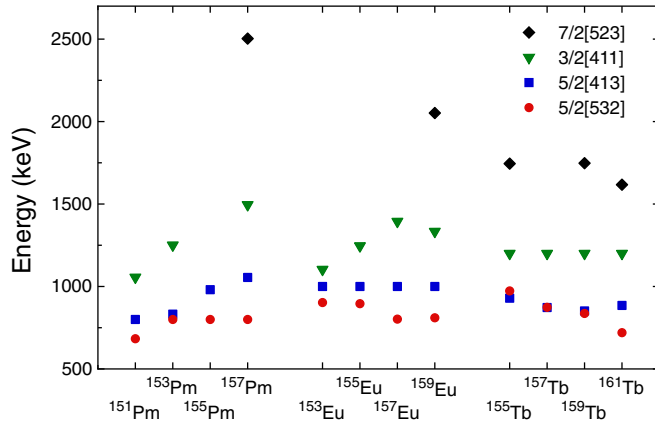


FIG. 5. Relative energies of quasiproton orbitals observed in promethium, europium, and terbium $N = 90, 92, 94,$ and 96 nuclei. The ground states were arbitrarily set at $800, 1000,$ and 1200 keV, respectively. Note that orbitals that lie below the ground-state configuration in a Nilsson diagram are shown at a lower energy relative to the ground state. The data for the nuclei (other than ^{157}Pm) were compiled from the National Nuclear Data Center, in particular from Refs. [13,14,21–24].

expected to be near the Fermi surface, and an assignment of the 695 -keV state to this orbital does follow the systematics seen in the nearby isotopes. Therefore, the $\pi 3/2[411]$ assignment is tentatively given to this level, and the 750 -keV state may be the first rotational excitation of this band as the energy difference (54 keV) is very similar to the energy differences observed between the $3/2$ and $5/2$ states of the $\pi 3/2[411]$ band in ^{159}Eu (58 keV) [13] and ^{161}Tb (56 keV) [14]. It should be noted, however, that the $\pi 3/2[541]$ assignment for the 695 -keV level cannot be unambiguously eliminated; although, the involved $\nu 5/2[523] \rightarrow \pi 3/2[541]$ decay would be hindered, since it would be a $\Delta n_z = \Delta \Lambda = 2$ forbidden transition.

Assignments for the states above 1 MeV are difficult to make based on the current data. However, the relatively low $\log ft \approx 4.8$ value for the 1703 -keV level does lead to a particular orbital assignment. When using the standard Nilsson notation of $K^\pi [Nn_z\Lambda]$, allowed-unhindered spin-flip β -decay transitions [25] occur between levels that obey the following

selection rules: $\Delta K = 1, \Delta N = 0, \Delta n_z = 0,$ and $\Delta \Lambda = 0$. They are associated with low $\log ft$ values (≤ 5.2) and are well known in this mass region, as summarized in Ref. [26]. Since the β -decaying state in ^{157}Nd is based on the $5/2[523]$ neutron orbital, a spin-flip decay would populate the state associated with the $7/2[523]$ proton orbital. This suggests that the 1703 -keV level has $J^\pi = (7/2^-)$, which is consistent with the observed decays into the $(5/2^-), (7/2^-),$ and $(5/2^+)$ states as seen in Fig. 4. Although the $\pi 7/2[523]$ orbital is not commonly observed in nearby nuclei, one can see from the systematics shown in Fig. 5 that its placement at 1703 keV in ^{157}Pm is consistent with the few available data points. That is, as the proton Fermi surface decreases from terbium to promethium, the $\pi 7/2[523]$ orbital lies at increasingly higher excitation energies.

V. SUMMARY

The neutron-rich ^{157}Nd nucleus was observed from an isobarically separated, $A = 157$ beam provided by the CARIBU source at Argonne National Laboratory. A half-life of $1.17(4)$ s was measured for the ground-state decay, which is in good agreement with the only other published value [10]. Transitions from the daughter ^{157}Pm isotope were identified and a level scheme has been presented. At low spin, states likely being based on the $\pi 5/2[532], \pi 5/2[413],$ and $\pi 3/2[411]$ proton orbitals were observed which match excitation-energy systematics from nearby promethium, europium, and terbium nuclei. Based on an unusually low ≈ 4.8 $\log ft$ value, the state at 1703 keV has been assigned the $\pi 7/2[523]$ configuration, as this decay is characteristic of an allowed-unhindered spin-flip β transition.

ACKNOWLEDGMENTS

This work is funded by the National Science Foundation under Grant No. PHY-2208137 (USNA), by the U.S. Department of Energy, Office of Nuclear Physics, under Contract No. DE-AC02-06CH11357 (ANL), and by the U.S. Department of Energy, National Nuclear Security Administration, Office of Defense Nuclear Nonproliferation R&D (NA-22). This research used resources of Argonne National Laboratory's ATLAS facility, which is a DOE Office of Science User Facility.

- [1] G. Savard, S. Baker, C. Davids, A. Levand, E. Moore, R. Pardo, R. Vondrasek, B. Zabransky, and G. Zinkann, *Nucl. Instrum. Methods Phys. Res. B* **266**, 4086 (2008).
- [2] R. Orford, N. Vassh, J. A. Clark, G. C. McLaughlin, M. R. Mumpower, G. Savard, R. Surman, A. Aprahamian, F. Buchinger, M. T. Burkey, D. A. Gorelov, T. Y. Hirsh, J. W. Klimes, G. E. Morgan, A. Nystrom, and K. S. Sharma, *Phys. Rev. Lett.* **120**, 262702 (2018).
- [3] R. Orford, F. G. Kondev, G. Savard, J. A. Clark, W. S. Porter, D. Ray, F. Buchinger, M. T. Burkey, D. A. Gorelov, D. J. Hartley, J. W. Klimes, K. S. Sharma, A. A. Valverde, and X. L. Yan, *Phys. Rev. C* **102**, 011303(R) (2020).
- [4] R. Orford, N. Vassh, J. A. Clark, G. C. McLaughlin, M. R. Mumpower, D. Ray, G. Savard, R. Surman, F. Buchinger, D. P. Burdette, M. T. Burkey, D. A. Gorelov, J. W. Klimes, W. S. Porter, K. S. Sharma, A. A. Valverde, L. Varriano, and X. L. Yan, *Phys. Rev. C* **105**, L052802 (2022).
- [5] D. J. Hartley, F. G. Kondev, R. Orford, J. A. Clark, G. Savard, A. D. Ayangeakaa, S. Bottoni, F. Buchinger, M. T. Burkey, M. P. Carpenter, P. Copp, D. A. Gorelov, K. Hicks, C. R. Hoffman, C. Hu, R. V. F. Janssens, J. W. Klimes, T. Lauritsen, J. Sethi, D. Seweryniak *et al.*, *Phys. Rev. Lett.* **120**, 182502 (2018).
- [6] R. Surman, J. Engel, J. R. Bennett, and B. S. Meyer, *Phys. Rev. Lett.* **79**, 1809 (1997).
- [7] M. R. Mumpower, G. C. McLaughlin, and R. Surman, *Phys. Rev. C* **85**, 045801 (2012).
- [8] M. R. Mumpower, G. C. McLaughlin, and R. Surman, *Phys. Rev. C* **86**, 035803 (2012).

- [9] M. R. Mumpower, G. C. McLaughlin, R. Surman, and A. W. Steiner, *J. Phys. G: Nucl. Part. Phys.* **44**, 034003 (2017).
- [10] J. Wu *et al.*, *Phys. Rev. Lett.* **118**, 072701 (2017).
- [11] A. J. Mitchell *et al.*, *Nucl. Instrum. Methods Phys. Res. A* **763**, 232 (2014).
- [12] S. Bhattacharyya, E. H. Wang, A. Navin, M. Rejmund, J. H. Hamilton, A. V. Ramayya, J. K. Hwang, A. Lemasson, A. V. Afanasjev, Soumik Bhattacharya, J. Ranger, M. Caamaño, E. Clément, O. Delaune, F. Farget, G. de France, B. Jacquot, Y. X. Luo, Yu. Ts Oganessian, J. O. Rasmussen, G. M. Ter-Akopian *et al.*, *Phys. Rev. C* **98**, 044316 (2018).
- [13] C. W. Reich, *Nucl. Data Sheets* **113**, 157 (2012).
- [14] C. W. Reich, *Nucl. Data Sheets* **112**, 2497 (2011).
- [15] N. B. Gove and M. J. Martin, *At. Data Nucl. Data Tables* **10**, 205 (1971).
- [16] M. Wang, W. J. Huang, F. G. Kondev, G. Audi, and S. Naimi, *Chin. Phys. C* **45**, 030002 (2021).
- [17] F. G. Kondev, ENSDF (2017), <https://doi.org/10.18139/nndc.ensdf/1845010>.
- [18] F. G. Kondev, M. Wang, W. J. Huang, S. Naimi, and G. Audi, *Chin. Phys. C* **45**, 030001 (2021).
- [19] C. W. Reich and B. Singh, *Nucl. Data Sheets* **111**, 1211 (2010).
- [20] B. Singh, ENSDF (2021), <https://doi.org/10.18139/nndc.ensdf/1845010>.
- [21] N. Nica, *Nucl. Data Sheets* **170**, 1 (2020).
- [22] N. Nica, *Nucl. Data Sheets* **160**, 1 (2019).
- [23] N. Nica, *Nucl. Data Sheets* **132**, 1 (2016).
- [24] B. Singh, *Nucl. Data Sheets* **110**, 1 (2009).
- [25] M. E. Bunker and C. W. Reich, *Rev. Mod. Phys.* **43**, 348 (1971).
- [26] P. C. Sood and R. K. Sheline, *At. Data Nucl. Data Tables* **43**, 259 (1989).